Synthesis, Structures, and Reactivity of Two Compounds Containing the Tancoite-like $[Ga(HPO_4)_2F]^{2-}_\infty$ Chain

Richard I. Walton, Franck Millange, and Dermot O'Hare*

Inorganic Chemistry Laboratory, University of Oxford, South Parks Road, Oxford, OX1 3QR, U.K.

Capucine Paulet, Thierry Loiseau, and Gérard Férey*

Institut Lavoisier, UMR CNRS 8637, Université de Versailles St Quentin en Yvelines, 45 Avenue des Etats-Unis, 78035 Versailles Cedex, France

Received March 2, 2000. Revised Manuscript Received May 2, 2000

Compounds containing the one-dimensional macroanion $[Ga(HPO_4)_2F]^{2-}$ have been synthesized using ambient and moderate solvothermal conditions, and their interconversion and reactivity studied. The anionic chains exist in the hydrated gallium fluorophosphate **(1)** $Ga(HPO_4)_2F\cdot(NH_3(CH_2)_3NH_3)\cdot 2H_2O$, synthesized at room temperature from an aqueous reaction. Heating **1** in air at 70 °C gives the dehydrated form **2** or $Ga(HPO_4)_2F\cdot(NH_3(CH_2)_3NH_3)$. **2** can also be solvothermally prepared at 120 °C from a water/DMF mixture and has been characterized by single-crystal X-ray diffraction. It is orthorhombic (space group *Pbcm* (no. 57), $a = 8.642(2)$ Å, $b = 19.346(13)$ Å, $c = 7.114(4)$ Å, $V = 1189.3(11)$ Å^3), and refined to $R1(F) = 0.0384$ and $wR2(F^2) = 0.0704$ for reflections with $I > 2\sigma(I)$. Both the structures contain anionic chains of corner-sharing GaO_4F_2 octahedra linked together via fluorine and PO_4 tetrahedra, the topology of which is the same as in the aluminophosphate mineral tancoite. Both **1** and **2** when heated with water under hydrothermal conditions produce the open-framework, three-dimensional phase ULM-3 without addition of any other reagents. This process has been followed in situ with time-resolved energy-dispersive diffraction, which reveals that dissolution of the one-dimensional phase occurs before the rapid crystallization of ULM-3.

Introduction

The research for novel microporous materials is very intense due to their industrial applications in the area of catalysis, sorption, ion-exchange processes, and gas separation[1]. Zeolites[2] (aluminosilicates and related pure silicates) and aluminophosphates[3] are the best known families exhibiting such properties. During the past decade, the synthesis of new three-dimensional architectures (inorganic or hybrid organic−inorganic) incorporating a wide range of elements (more than 40 up to now) has increased drastically the number of potential porous materials.[4] Most of them are prepared under mild hydrothermal conditions ($T < 200$ °C, autogenous pressure) by means of an organic template (amine or tetralkylammonium salt) or a functionalized organic ligand (phosphonates, carboxylates, for example). Despite the richness of the crystal chemistry of the open-framework solids, rational design of new materials is still not possible, and much postulation of reaction mechanism has taken place. For example, Ozin and co-workers have proposed a model for the formation of microporous aluminophosphates based on the existence of a linear chain aluminophosphate which would play the role of building block.[5] Through hydrolysis−condensation reactions, the components of the chain aluminophosphates may reassemble in solution to precipitate layered and three-dimensional networks.[5] Rao et al. have reported the formation of amine phosphates which may be a precursor for the elaboration of the three-dimensional zinc phosphates,[6] and Férey proposed a reaction scheme based on the charge density matching between the structure-directing agent (amine) and the inorganic oligomeric building species, which may occur in the solution during the formation of fluorinated phosphates.[7] These models are still lacking experimental proof, although recent in situ NMR experiments on the phosphate AlPO4-CJ2[8] and on porous titanium(IV) phosphates[9] showed the existence of tetrameric units in solution, consistent with the crystallization model of Férey.

(1) Venuto, P. *Microporous Mater.* **1994**, *2*, 297.
(2) Breck, D. W. *Zeolite Molecular Sieves: Structure, Chemistry and Use*; Wiley and Sons: London, 1974.
(3) Wilson, S. T.; Lok, B. M.; Messina, C. A.; Cannon, T. R.; Flanigen, E. M. *J. Am. Chem. Soc.* **1982**, *104*, 1146.
(4) Cheetham, A. K.; Férey, G.; Loiseau, T. A*ngew. Chem., Int. Ed.* **1999**, *38*, 3268.
(5) Oliver, S.; Kuperman, A.; Ozin, G. A. *Angew. Chem., Int. Ed.* **1998**, *37*, 46.
(6) Neeraj, S.; Natarajan, S.; Rao, C. N. R. *Angew. Chem., Int. Ed.* **1999**, *38*, 3480.
(7) Férey, G. *J. Fluorine Chem.*, **1995**, *72*, 187; Férey, G. *C. R. Acad. Sci. Paris, Ser. IIc*, **1998**, *1*, 1.
(8) Taulelle, F.; Haouas, M.; Gerardin, C.; Estournes, C.; Loiseau, T.; Férey G. *Colloids Surf., A* **1999**, *158*, 299.
(9) Serre, C.; Taulelle, F.; Férey, G. Manuscript in preparation.

10.1021/cm000195+ CCC: $19.00
Published on Web 06/23/2000

Table 1. Reactions Performed in the Current Work

composition of the starting mixture	reaction conditions	product[a]
Ga_2O_3:2H_3PO_4:1.9DAP:2.1HF:70H_2O	25 °C, 1 week	$Ga(HPO_4)_2F{\cdot}H_3N(CH_2)_3NH_3{\cdot}2H_2O$ **(1)** + GaOOH + β-Ga_2O_3
Ga_2O_3:4H_3PO_4:3.6DAP:4HF:70H_2O	25 °C, 1 week	$Ga(HPO_4)_2F{\cdot}H_3N(CH_2)_3NH_3{\cdot}2H_2O$ **(1)** + GaOOH (trace)
Ga_2O_3:2H_3PO_4:1.9DAP:70H_2O	25 °C, 1 week	$[H_3N(CH_2)_3NH_3][HPO_4]{\cdot}H_2O$ (ref 17) + GaOOH + β-Ga_2O_3
GaO(OH):H_3PO_4:0.5DAP:7.4DMF:4.4H_2O	hydrothermal, 120 °C, 3 days	$Ga(HPO_4)_2F{\cdot}H_3N(CH_2)_3NH_3$ **(2)** (single crystals) + MIL-30 (trace)[b]

[a] Product identification by powder X-ray diffraction. [b] MIL-30 is a layered gallium fluorophosphate (see the text).

In situ characterization of chemical reactions is important for a complete understanding of the roles of the different parameters (reactants, temperature, time, etc.) during the synthesis.[10] Besides the NMR measurements mentioned above, we recently reported in situ measurements of the hydrothermal preparation of open-framework phosphates by means of time-resolved energy-dispersive X-ray diffraction (EDXRD) using synchrotron radiation. We observed the formation of intermediate phases during the synthesis of the fluorinated gallium phosphates ULM-5[11] and ULM-3[12] when H_3PO_4 was replaced by P_2O_5 as phosphorus source. To gain information on the nature of the intermediate phases, we are currently investigating the possibility of isolating crystalline precursors of these phases under ambient conditions. We recently described a preliminary account of room-temperature crystallization of a chain gallium fluorophosphate, $Ga(HPO_4)_2F{\cdot}(NH_3(CH_2)_3NH_3){\cdot}2H_2O$.[13] This material forms from the reaction mixture which, if treated hydrothermally, leads to the previously known three-dimensional networks ULM-3[14] and ULM-4.[15] We now describe the thermal behavior of the one-dimensional gallium fluorophosphate and its hydrothermal conversion into ULM-3. We have also prepared an anhydrous form of the compound by a mild hydrothermal route as single crystals, and its structure is shown to be related to that of the fluorinated iron phosphate ULM-14.[16]

Experimental Section

Synthesis and Structural Characterization. Syntheses were carried out at room temperature or under mild hydrothermal conditions using gallium oxide (Ga_2O_3, 99.99%, Aldrich) or gallium oxyhydroxide (GaO(OH), prepared by the hydrothermal reaction of gallium metal with water), phosphoric acid (H_3PO_4, 85% in water Prolabo), hydrofluoric acid (HF, 40%, Prolabo), 1,3-diaminopropane ($H_2N(CH_2)_3NH_2$, 99%, Aldrich), denoted DAP, dimethylformamide ($(CH_3)_2NCHO$, 99.8%, SDS), denoted DMF, and deionized water. Table 1 shows the initial compositions of reaction mixtures used and the conditions applied.

$Ga(HPO_4)_2F{\cdot}(NH_3(CH_2)_3NH_3){\cdot}2H_2O$ (**1**) crystallizes after one week at room temperature from a reaction mixture usually heated under hydrothermal conditions to produce the open-framework gallium fluorophosphate ULM-3. We have recently reported the details of the synthesis and structure analysis of **1**.[13] Interestingly, if HF was omitted from the reaction mixture, the only crystalline phase identified was 1,3-propanediammonium phosphate hydrate.[17] This amine phosphate was never observed to form in any other reaction studied.

The anhydrous gallium fluorophosphate $Ga(HPO_4)_2F{\cdot}(NH_3(CH_2)_3NH_3)$ **(2)** was prepared as single crystals under mild hydrothermal conditions using a mixed water/DMF solvent (Table 1). A 0.713 g sample of GaO(OH), 0.5 mL of H_3PO_4, 0.2 mL of HF, 0.3 mL of DAP, 4 mL of DMF, and 0.3 mL of H_2O were sealed in a Teflon-lined autoclave and heated at 120 °C for 3 days. The white solid product was recovered by filtration, washed with deionized water, and dried at room temperature. Traces of MIL-30, a lamellar phase which also crystallizes from the $Ga_2O_3-H_3O_4-H_2O-HF-DAP-DMF$ system,[18] were observed with **2** by powder X-ray diffraction. A single crystal of **2** was carefully selected under a polarizing microscope and glued onto a glass fiber. Intensity data were recorded on a Siemens SMART three-circle diffractometer equipped with a CCD bidimensional detector (Mo Kα radiation). The crystal-to-detector distance was 45 mm, allowing for data collection up to 60° (2θ). Slightly more than one hemisphere of data were recorded, and the acquisition time per frame was 30 s with a scan width of 0.3° in ω. An empirical absorption correction was applied using the SADABS program.[19] The structure of the gallium phosphate was solved and refined using SHELXTL[20] in the standard space group *Pbcm*. The gallium and phosphorus atoms were located by direct methods and all the other non-hydrogen atoms (F, O, C, N) placed from subsequent Fourier-difference map calculations. The hydrogen atoms belonging to the organic molecule were placed with geometrical restraints and refined isotropically, and those by the two phosphate groups were located from the examination of the Fourier-difference map. With this model, the reliability factors are $R1(F) = 0.0384$ and $wF(F^2) = 0.0704$ for reflections $I > 2\sigma(I)$. The chemical formula deduced from the crystal structure is $Ga(HPO_4)_2F{\cdot}N_2C_3H_{12}$. Fluorine analysis, performed using a potentiometric method with a flouride ion selective electrode, is in good agreement with this formula (F/P = 0.53 (expected 0.50)). Crystal data and details of the data collection are summarized in Table 2. The resulting atomic coordinates, selected bond distances and angles, and positions of hydrogen atoms of **2** are listed in Tables 3 and 4.

Powder X-ray Diffraction. A number of powder X-ray diffraction methods were used to characterize the materials. Variable-temperature powder X-ray diffraction measurements were performed using a Siemens D5000 diffractometer (Cu Kα radiation) equipped with an Anton Paar furnace (HTK1200) under a flow of wet He. The diffractometer was used in reflection mode, and data were measured over the angular range $2\theta = 5-25°$ to observe the most intense low-angle Bragg reflections. Temperature steps of 10 °C were typically used,

(10) Cheetham, A. K.; Mellot, C.F. *Chem. Mater.* **1997**, *9*, 2269.
(11) Francis, R. J.; Price, S. J.; O'Brien, S.; Fogg, A. M.; O'Hare, D.; Loiseau, T.; Férey, G. *Chem. Commun.* **1997**, *521*. Francis, R. J.; Fogg, A. M.; O'Brien, S.; Halasyamani, P. S.; O'Hare, D.; Loiseau. T.; Férey, G. *J. Am. Chem. Soc.* **1999**, *121*, 1002.
(12) Walton, R. I.; Loiseau, T.; O'Hare, D.; Férey, G. *Chem. Mater.* **1999**, *11*, 3201.
(13) Walton, R. I.; Millange, F.; Le Bail, A.; Loiseau, T.; Serre, C.; O'Hare, D.; Férey, G. *Chem. Commun.* **2000**, 203.
(14) Loiseau, T.; Retoux, R.; Lacorre, P.; Férey, G. *J. Solid State Chem.* **1994**, *111*, 427.
(15) Loiseau, T.; Taulelle, F.; Férey, G. *Microporous Mater.* **1997**, *9*, 83.
(16) Cavellec, M.; Riou, D.; Grenèche; J−M.; Férey, G. *Inorg. Chem.* **1997**, *36*, 2187.
(17) Kamoun, S.; Jouini, A.; Daoud, A. *Acta Crystallogr., C* **1991**, *47*, 117.
(18) Paulet, C.; Loiseau. T.; Férey, G. *J. Mater. Chem.* **2000**, *10*, 1225.
(19) M. Sheldrick, SADABS program: Siemens Area Detector ABSorption corrections, G. unpublished work.
(20) G. M. Sheldrick, SHELXTL version 5.03, Siemens Analytical X-ray Instrument, Madison, WI, 1994.

Table 2. Experimental and Crystallographic Parameters for the Structure Analysis of $GaF(HPO_4)_2 \cdot N_2C_3H_{12}$ (2)

empirical formula	$C_3H_{14}FGaN_2O_8P_2$	cryst size (mm)	0.66 × 0.04 × 0.02
fw	356.82	θ range for data collection (deg)	2.11−29.88
temp (K)	296(2)	limiting indices	$-11 \le h \le 10$, $-26 \le k \le 26$, $-6 \le l \le 9$
wavelength (Å)	0.710 73	reflns collected	7919
cryst system	orthorombic	no. of independent reflns	1696 [R(int) = 0.0705]
space group	*Pbcm* (no. 57)	refinement method	full-matrix least-squares on F^2
unit cell dimensions (Å)	a = 8.642(2)	no. of data/restraints/params	1149/0/106
	b = 19.346(13)	goodness-of-fit on $F2$	1.040
	c = 7.114(4)	final R indices [$I > 2\sigma(I)$]	R1 = 0.0384, wR2 = 0.0704
vol (Å^3), Z	1189.3(11), 4	R indices (all data)	R1 = 0.0760, wR2 = 0.0835
density (calcd) (g/cm^3)	1.993	extinction coeff	0.0020(4)
abs coeff (mm^{-1})	2.628	largest diff peak and hole (e·Å^{-3})	0.617 and −0.466
F(000)	720		

Table 3. Atomic Coordinates (×10^4) and Equivalent Isotropic Displacement Parameters (Å^2 × 10^3) for 2

atom	x	y	z	U(eq)[a]
Ga(1)	5000	0	0	14(1)
P(1)	6511(1)	1217(1)	2500	17(1)
P(2)	2344(1)	766(1)	2500	17(1)
F(1)	5217(3)	−412(1)	2500	17(1)
O(1)	8221(4)	1487(2)	2500	25(1)
O(2)	6260(3)	782(1)	738(3)	31(1)
O(3)	630(4)	645(2)	2500	27(1)
O(4)	3124(3)	470(1)	741(3)	28(1)
O(5)	2556(5)	1572(2)	2500	41(1)
O(6)	5533(4)	1861(2)	2500	46(1)
N(1)	1288(5)	−504(2)	2500	27(1)
N(2)	3647(5)	1778(2)	2500	27(1)
C(1)	1929(6)	1844(3)	2500	30(1)
C(2)	1137(6)	1146(3)	2500	30(1)
C(3)	−567(6)	1202(3)	2500	39(2)
H(1)	8855(76)	1223(31)	2500	53(23)
H(2)	3339(60)	1673(27)	2500	21(17)

[a] U(eq) is defined as as one-third of the trace of the orthogonalized U_{ij} tensor.

and the temperature was stabilized for 5 min before data collection was begun at each step. Station 2.3 of the Daresbury SRS was used to perform high-resolution powder X-ray diffraction studies. Station 2.3 receives X-ray from the synchrotron (which operates with an average energy of 2 GeV and a typical beam current of 200 mA) from a dipole insertion device. For our experiments, the incident X-ray wavelength was 1.3005 Å, selected using a Si(111) monochromator, and data were collected from a sample contained in a thin-walled 0.7 mm diameter glass capillary. Station 16.4 of the Daresbury SRS was used to perform time-resolved energy-dispersive X-ray diffraction (EDXRD) studies. The high-intensity ($\sim 10^{10}$ photons s^{-1}) white X-ray beam (5−120 keV) allows the penetration of thick-walled reaction vessels, and the fixed detector provides rapid data acquisition (<1 min). Thus, in situ time-resolved diffraction studies of chemical processes are possible under genuine laboratory conditions, and a hydrothermal reaction cell for such studies has previously been described.[21] This apparatus was used for the current work. Diffraction data were recorded every 30 s by a detector fixed at 1.88°. In the energy-dispersive experiment E(keV) = 6.19926/(d sin θ) for a Bragg reflection arising from a plane of d (Å) observed in a detector fixed at 2θ°.

Thermogravimetry. Thermogravimetric analysis was carried out either on a TA Instrument type 2050 thermoanalyzer under nitrogen gas flow with a heating rate of 5 °C·min^{-1} from 25 to 1050 °C or using a Rheometric Scientific STA 1500 instrument, under flowing air, with a heating rate of 5 °C·min^{-1} from 25 to 1000 °C.

Results

Structure Description. The single-crystal structure reveals that **2** is isostructural with a previously characterized iron(III) phosphate, ULM-14 (a = 7.221 Å, b = 8.655 Å, c = 19.329 Å, space group *Pmca*).[16] Its structure contains anionic chains $[Ga(HPO_4)_2F]^{2-}$ separated by charge-balancing 1,3-propanediammonium cations (Figure 1). The chains are constructed from GaO_4F_2 octahedra sharing trans (F) vertexes running along [001]. The gallium octahedron is slightly distorted, the Ga−O distances (average Ga−O = 1.934(2) Å) being shorter than the Ga−F distances (Ga−F = 1.957(1) Å). The four oxygen atoms are shared with phosphate groups, and the octahedra making up the spine of the chain are tilted in such a way that each phosphate group links two adjacent octahedra (Figure 2). The two crystallographically distinct phosphorus atoms are tetrahedrally coordinated with P−O distances ranging from 1.50 to 1.57 Å. For each phosphate group, a longer P−O distance is observed (P(1)−O(1) = 1.567(3) Å and P(2)−O(5) = 1.568(4) Å), indicating the presence of a hydroxyl group (P−OH). The remaining free vertex is occupied by a phosphoryl P═O group (P(2)−O(3) = 1.500(3) Å and P(1)−O(6) = 1.505(4) Å). The diaminopropane molecules lie between the resulting chains $[Ga(HPO_4)_2F]^{2-}$ and are protonated twice for balancing the two negative charges of the inorganic chain. Several kinds of hydrogen-bonding interactions occur in the structure (Figure 3a) and are responsible for the cohesion of the chains. Two adjacent chains are linked via the hydroxyl groups of P(1)O(1)H(1) and terminal bond P(2)−O(3) (O(1)H(1)···O(3) = 1.899(1) Å). This connection is strengthened by the presence of the ammonium group N(1), which is hydrogen-bonded with O(3) ((N(1)···O(3) = 2.771(1) Å), O(4) (N(1)···O(4) = 2.800(1) Å), and F(1) (N(1)···F = 3.026(1) Å). The other ammonium group N(2) interacts with anions belonging to two other adjacent chains and ensures the cohesion of the solid (N(2)···O(6) = 2.727-(2) Å, N(2)···O(2) = 3.004(1) Å, N(2)···F = 2.971(2) Å). Additional intrachain hydrogen bond interactions occur between the hydroxyl group O(5)H(2) and the terminal P−O(6).

The topologies of the chains in compounds **1** and **2** are identical, but the arrangements of the chains in the two compounds are slightly different since in the hydrated form, two water molecules are found between the chains. Figure 3b shows the hydrogen bonding observed in **1**. Two adjacent chains still interact together by hydrogen bonds from the hydroxyl groups and terminal P═O bonds and via one of the two ammonium groups of the diamine. The three-dimensional cohesion of the structure is ensured by both the other ammonium group of diamine and the water molecule interacting with the P−O or Ga−F. The presence of water molecules slightly modifies the chain packing, which is more

(21) Evans, J. S. O.; Francis, R. J.; O'Hare, D.; Price, S. J.; Clarke, S. M.; Flaherty, J.; Gordon, J.; Nield, A.; Tang, C. C. *Rev. Sci. Instrum.* **1995**, *66*, 2442.

Table 4. Principal Bond Lengths (Å) and Angles in $Ga(HPO_4)_2F{\cdot}H_3N(CH_2)_3NH_3$ (2)

Ga(1)−O(4)	1.932(2)	P(1)−O(1)	1.567(3)	N(2)−C(1)	1.490(6)
Ga(1)−O(2)	1.936(2)	P(2)−O(3)	1.500(3)	C(1)−C(2)	1.515(7)
Ga(1)−F(1)	1.9575(14)	P(2)−O(4)	1.533(3)	C(2)−C(3)	1.477(7)
P(1)−O(6)	1.505(4)	P(2)−O(5)	1.568(4)		
P(1)−O(2)	1.525(3)	N(1)−C(3)	1.487(6)		
O(4)−Ga(1)−O(4)#1	180.0	O(4)−Ga(1)−F(1)	91.39(10)	O(2)#2−P(1)−O(1)	108.55(13)
O(4)−Ga(1)−O(2)	91.71(12)	O(4)#1−Ga(1)−F(1)	88.61(10)	O(3)−P(2)−O(4)#2	112.05(12)
O(4)#1−Ga(1)−O(2)	88.29(12)	O(2)#1−Ga(1)−F(1)#1	91.00(10)	O(3)−P(2)−O(4)	112.05(12)
O(4)−Ga(1)−O(2)#1	88.29(12)	O(2)#1−Ga(1)−F(1)	89.00(10)	O(4)#2−P(2)−O(4)	109.5(2)
O(4)#1−Ga(1)−O(2)#1	91.71(12)	F(1)#1−Ga(1)−F(1)	180.0	O(3)−P(2)−O(5)	105.7(2)
O(2)−Ga(1)−O(2)#1	180.0	O(6)−P(1)−O(2)	112.12(13)	O(4)#2−P(2)−O(5)	108.67(13)
O(4)−Ga(1)−F(1)#1	88.61(10)	O(6)−P(1)−O(2)#2	112.12(13)	O(4)−P(2)−O(5)	108.67(13)
O(4)#1−Ga(1)−F(1)#1	91.39(10)	O(2)−P(1)−O(2)#2	110.5(2)	N(2)−C(1)−C(2)	111.9(4)
O(2)−Ga(1)−F(1)#1	89.00(10)	O(6)−P(1)−O(1)	104.7(2)	C(3)−C(2)−C(1)	112.6(4)
O(2)#1−Ga(1)−F(1)#1	91.00(10)	O(2)−P(1)−O(1)	108.55(13)	C(2)−C(3)−N(1)	110.5(4)

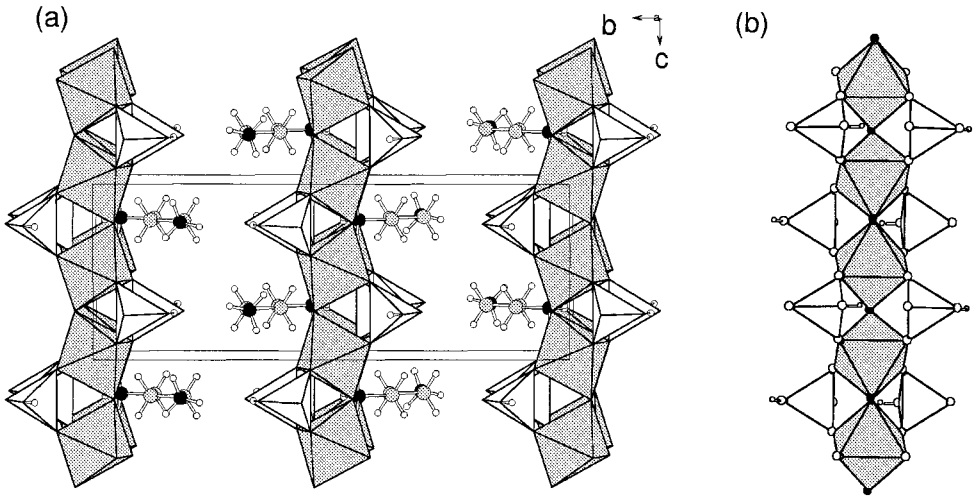

Figure 1. (a) Structure of $Ga(HPO_4)_2F{\cdot}H_3N(CH_2)_3NH_3$ **(2)** viewed along the *a* axis and (b) representation of the tancoite-type chain. Gray polyhedra are GaO_4F_2 octahedra, and white polyhedra, PO_4 tetrahedra.

distorted in the hydrated form and induces a lower symmetry. Indeed, cell parameters are closely related ($a_1 \approx b_2$, $b_1 \approx a_2$, $c_1 \approx b_2/2$), but in **1**, all the chains have the same orientation, whereas in **2**, they exhibit opposite rotations around the central carbon of diammoniumpropane. Moreover, in **1**, ammonium groups were hydrogen bonded to the water molecule. When the latter evolves the structure, a modification of the hydrogen-bonding scheme leads to the rotations cited above and also to a reorientation of the anions closer to the b_1 or a_2 direction (Figure 2).

The topology of the $[Ga(HPO_4)_2F]^{2-}$ chains has previously been reported for several other compounds, first in the mineral tancoite, $LiNa_2HAl(PO_4)_2(OH)$,[22] but also in synthetic aluminum and gallium phosphates[23−25] and in transition-metal phosphates.[16,26,27] It should be noted that the structures of the tancoite-like compounds are distinct from another group of one-dimensional aluminum and gallium phosphates prepared solvothermally (usually using alcoholic media) with composition $[Ga(PO_4)(HPO_4)^{2-}]$.[28−34] For the chains in these materials, which all also contain charge-balancing alkylammonium cations, the metals are found only in tetrahedral environments.

Thermal Behavior of the Materials. The TG curve of **2** shows two different weight losses (Figure 4a). After a slight continuous weight loss at low temperature (<200 °C, 0.92%), which is most likely due to absorbed water or solvent, the removal of the 1,3-diaminopropane molecule is observed between 200 and 600 °C (obsd 21.89%; calcd 21.87%). The final event at higher temperatures can be assigned to the departure of the fluorine (obsd 6.42%; calcd 5.3%). The XRD pattern of the residue at 1035 °C corresponds to dense gallium phosphate with the low cristobalite structure type together with an amorphous phase.

For **1** (Figure 4b) a first weight loss of 8.7% occurs between 50 and 90 °C and corresponds to the loss of occluded water (expected 9.1%). Between 300 and 700 °C a gradual mass loss of 22.3% is consistent with the

(22) Hawthorne, F. C. *Tschermaks Mineral. Petrogr. Mitt.* **1983**, *31*, 121.
(23) Attfield, M. P.; Morris, R. E.; Burshtein, I.; Campana, C. F.; Cheetham, A. K. *J. Solid State Chem.* **1995**, *118*, 412.
(24) Lii, K. H.; Wang, S. L. *J. Solid State Chem.* **1997**, *128*, 21.
(25) Lin, H. M.; Lii, K. H. *Inorg. Chem.* **1998**, *37*, 4220
(26) Lethbridge, Z. A. D.; Lightfoot, P.; Morris, R. E.; Wragg, D. S.; Wright, P. A.; Kvick, A.; Vaughan, G. *J. Solid State Chem.*, **1999**, *142*, 455.
(27) Zhang, Y.; Warren, C. J.; Clearfield, A.; Haushalter, R. C. *Polyhedron* **1998**, *17*, 2575
(28) Sugiyama, K.; Hiraga, K.; Yu, J.; Zheng, S.; Qiu, S.; Xu, R.; Terasaki, O. *Acta Crystallogr., C* **1999**, *55*, 1615.
(29) Yu, J.; Williams, I. D. *J. Solid State Chem.* **1998**, *136*, 141.
(30) Chippindale, A. M.; Turner, C. *J. Solid State Chem.* **1997**, *128*, 318.
(31) Gao, Q.; Chen, J.; Li, S.; Xu, R.; Thomas, J. M.; Light, M.; Hursthouse, M. B. *J. Solid State Chem.* **1996**, *127*, 145.
(32) Jones, R. H.; Thomas, J. M.; Xu, R.; Huo, Q.; Xu, Y.; Cheetham, A. K.; Bieber, D. *Chem. Commun.* **1990**, 1170.
(33) Loiseau, T.; Serpaggi, F.; Férey, G. *Chem. Commun.* **1997**, 1093.
(34) Chippindale, A. M.; Bond, A. D.; Law, A. D.; Cowley, A. R. *J. Solid State Chem.* **1998**, *136*, 227.

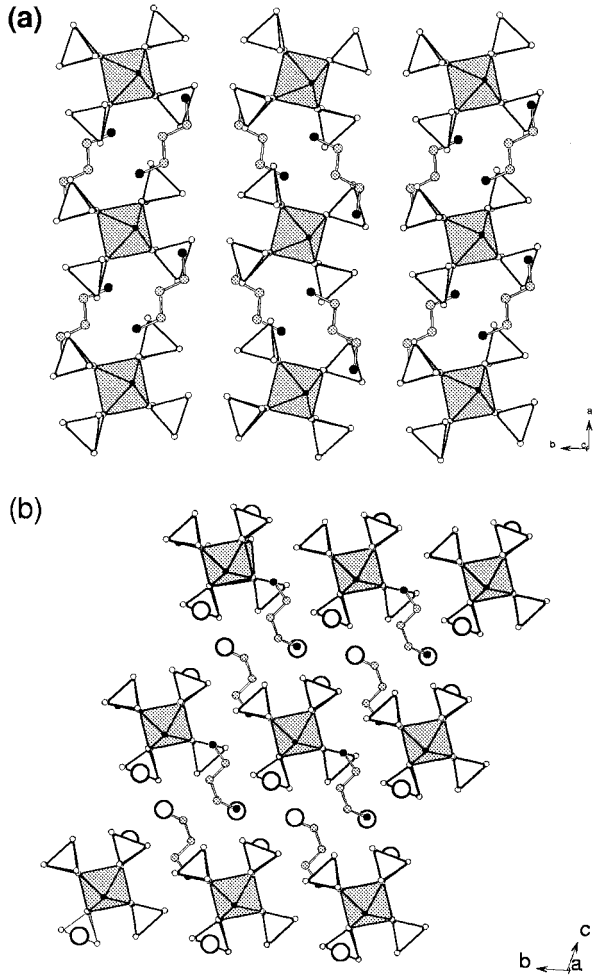

Figure 2. (a) Structure of $Ga(HPO_4)_2F{\cdot}H_3N(CH_2)_3NH_3$ **(2)** and (b) $Ga(HPO_4)_2F{\cdot}H_3N(CH_2)_3NH_3{\cdot}2H_2O$ **(1)** viewed, respectively, along the chain axes *c* and *a*.

loss of amine (expected 21.87%). The final mass loss above 700 °C may be ascribed to the loss of fluorine as before. Once the hydrated material has lost water, its thermal behavior is remarkably similar to that of **2**, and the final product as before is dense gallium phosphate ($GaPO_4$). The differences in temperature of each step for the two compounds may be attributed to different apparatuses and heating rates applied in these experiments.

Variable-temperature powder X-ray diffraction studies of **1** show that crystallinity is retained on loss of water (Figure 5). It was also observed that the transformation was readily reversible; after heating to 70 °C followed by cooling to room temperature, the powder X-ray diffraction pattern showed that some of the material had converted back to the starting phase. Because of preferred orientation when using the flat-plate geometry in this experiment, the low-angle reflections of the materials are artificially enhanced in intensity, making structural characterization and even identification of the dehydration product of **1** difficult. To gain more information, a finely ground sample of **1** was placed in a 0.7 mm glass capillary and dehydrated in situ by heating overnight at 70 °C. The capillary was sealed immediately on removal from the oven to avoid rehydration and synchrotron powder X-ray diffraction data measured on Station 2.3 of the Daresbury SRS (Figure 6). It is apparent from these high-resolution

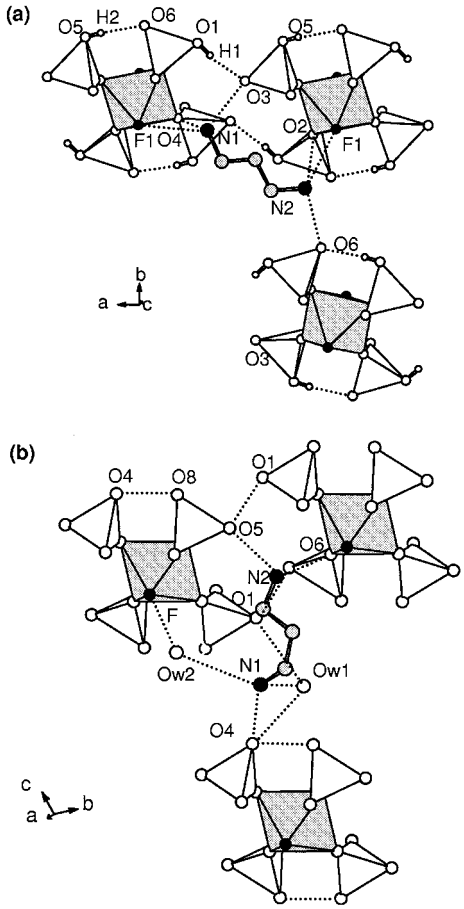

Figure 3. Hydrogen bonding in (a) $Ga(HPO_4)_2F{\cdot}H_3N(CH_2)_3NH_3$ **(2)** and (b) $Ga(HPO_4)_2F{\cdot}H_3N(CH_2)_3NH_3{\cdot}2H_2O$ **(1)**.

data that although the material was effectively dehydrated and rehydration avoided, loss of crystallinity occurs during the process. The large background and anisotropic broadening of Bragg reflections meant that the data were unsuitable for structural refinement. However, a comparison with the simulated X-ray diffraction pattern of **2** shows that the dehydrated phase exhibits a very similar diffraction pattern (Figure 6), and refinement of the cell parameters against the data confirms the structural similarity (a = 8.663 Å, b = 19.402 Å, c = 7.112 Å in *Pbcm*).

Hydrothermal Behavior of the Materials. The chain gallium fluorophosphates we have characterized contain the same protonated amine which has previously been observed as a charge-balancing and/or space-filling species in several other gallium fluorophosphates, including those with two-dimensional (lamellar) structures[18] and three-dimensional open-framework structures.[14,15,35] Given the interest in the conversion of low-dimensional phosphates to those with structures of higher dimensionality in relation to understanding the crystallization mechanism, we investigated the behavior of **1** under hydrothermal conditions. Experiments in the laboratory revealed that if the phase prepared at room temperature was placed in a hydrothermal autoclave with water (~0.5 g with 10 cm^3 water) and heated at 180 °C for 15 h, pure polycrystalline ULM-3 was produced with no crystalline impurity. ULM-3, Ga_3-

(35) Simon, N.; Loiseau, T.; Férey, G. *J. Chem. Soc., Dalton Trans.* **1999**, 1147.

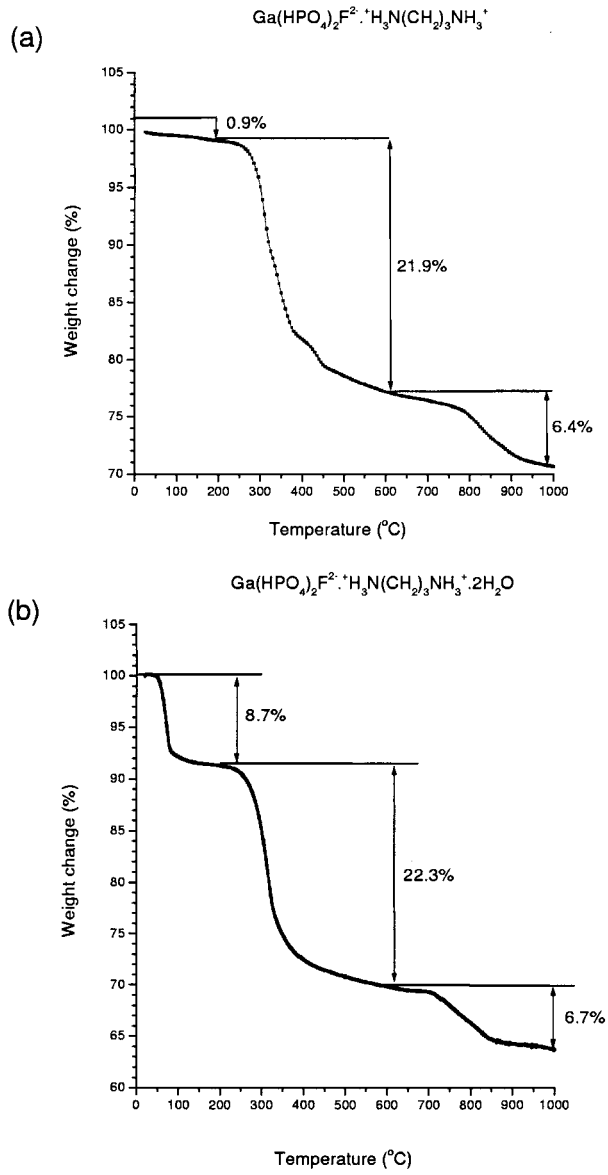

Figure 4. TGA traces for (a) $Ga(HPO_4)_2F{\cdot}H_3N(CH_2)_3NH_3$ (**2**), performed in dry nitrogen, and (b) $Ga(HPO_4)_2F.H_3N(CH_2)_3NH_3{\cdot}2H_2O$ **(1)**, performed in dry air.

$(PO_4)_3F_2{\cdot}H_3N(CH_2)_3NH_3{\cdot}H_2O$, is an open-framework three-dimensional gallium fluorophosphate constructed from GaO_4F_2 octahedra, GaO_4F trigonal bipyramids, and PO_4 tetrahedra.[14] It should be noted that no extra reagents were added to effect the transformation, and given that the Ga:P in ULM-3 is 1:1 and not 1:2 as in the chain compound, then we must assume the extra phosphorus must remain in solution. The pH of the supernatant liquid after the reaction was found to be ~3, consistent with the presence of phosphorus-oxy species. Exactly the same result was obtained when **2** was heated with water in an autoclave at 180 °C. In situ EDXRD was used to follow the transformation of **1** to ULM-3. Figure 7 shows diffraction data measured from the hydrothermal bomb as 0.5 g of $Ga(HPO_4)_2F{\cdot}(NH_3(CH_2)_3NH_3){\cdot}2H_2O$ was heated with 10 g of water and the temperature increased gradually to 180 °C. Integrated peak areas for single well-resolved Bragg reflections are shown in Figure 7b. This plot shows that the Bragg reflections of the chain phase disappear rapidly once a temperature of ~110 °C is reached and

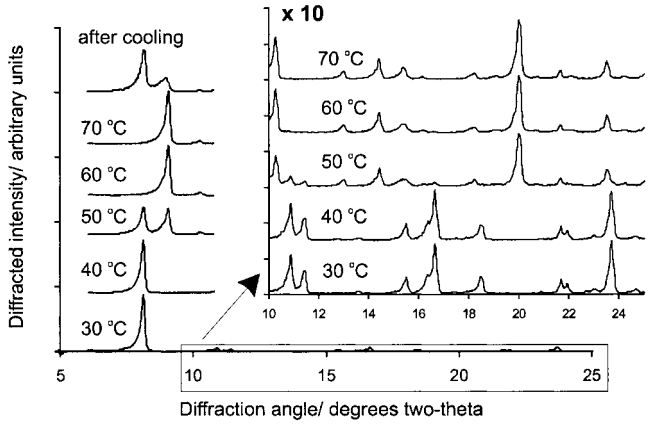

Figure 5. Variable-temperature powder X-ray diffraction patterns (Cu Kα radiation) recorded as $Ga(HPO_4)_2F{\cdot}H_3N(CH_2)_3NH_3{\cdot}2H_2O$ **(1)** was heated under He, and after cooling to room temperature. The inset shows an expanded portion of the high-angle region.

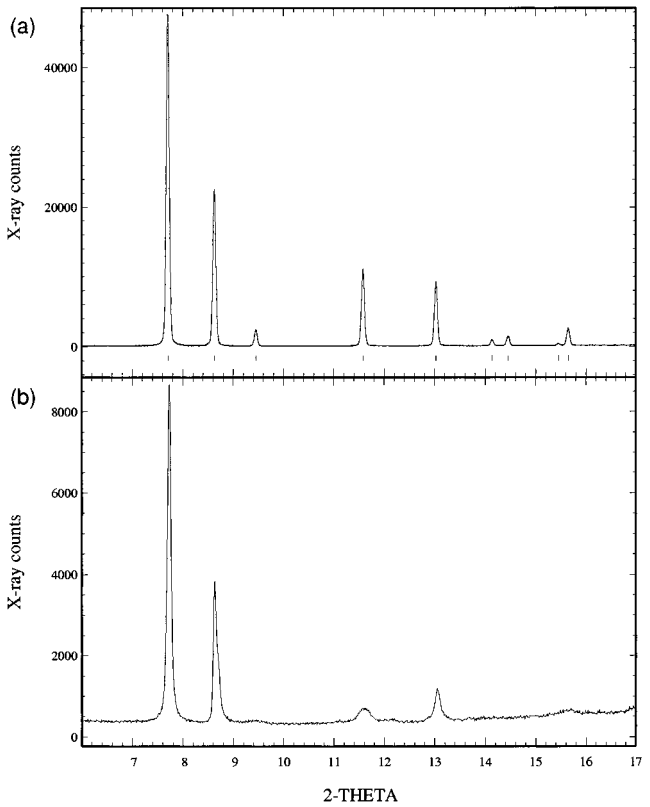

Figure 6. (a) Simulated powder X-ray diffraction pattern of $Ga(HPO_4)_2F{\cdot}H_3N(CH_2)_3NH_3$ **(2)** and (b) the pattern recorded from the dehydration product of $Ga(HPO_4)_2F{\cdot}H_3N(CH_2)_3NH_3{\cdot}2H_2O$ ($\lambda = 1.3005$ Å).

ULM-3 begins to crystallize after most of the starting material has dissolved. In addition, the stack plot (Figure 7a) shows the transient appearance of another crystalline phase before ULM-3 forms, with a strong Bragg reflection of *d* spacing 8.38 Å. At first glance, this diffraction signal might be assigned to 1,3-propanediammonium phosphate hydrate**,** which exhibits a characteristic highest *d* spacing peak of 8.32 Å.[17] However, this phase is expected to exhibit more intense reflections at lower *d* spacings, and no other Bragg reflections were observed in either of the other two detectors used in the EDXRD experiments. The dehydratation of **1** is not observed during the hydrothermal treatment, since the

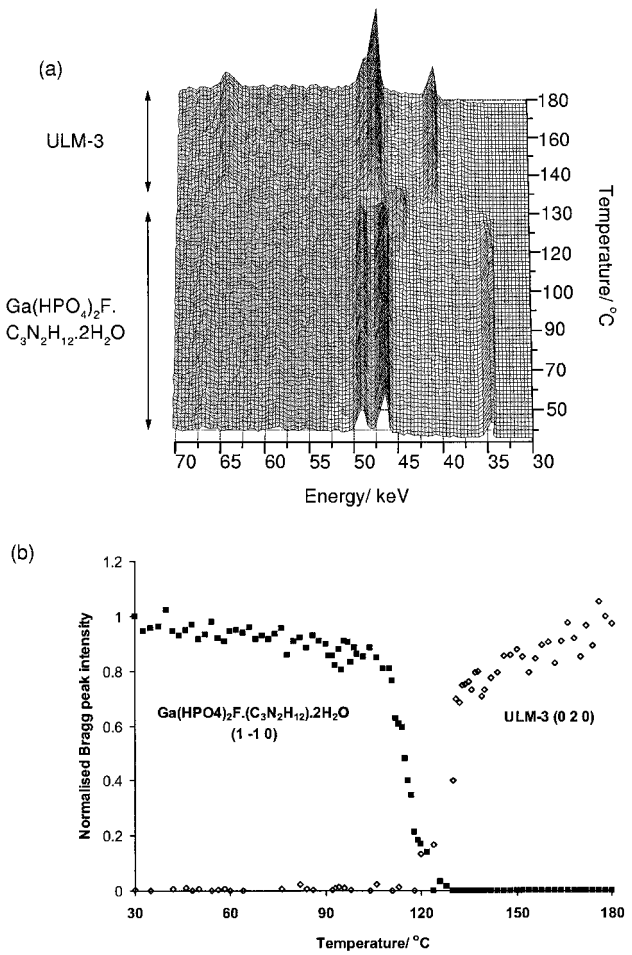

Figure 7. EDXRD data recorded in situ as $Ga(HPO_4)_2F{\cdot}H_3N(CH_2)_3NH_3{\cdot}2H_2O$ **(1)** is heated with water in the hydrothermal bomb: (a) a stack plot of the data and (b) peak intensities of the strongest Bragg reflections of **1** and ULM-3 as a function of temperature.

expected diffraction peak for **2** is not visible. The transient phase is present for less than 5 min total, making its identification very difficult. Quenching experiments were performed with the aim of isolating the transient, but always either the starting material or ULM-3 was recovered. Isothermal in situ EDXRD experiments were also performed with the aim of extending the lifetime of the transient phase, but its appearance was equally as brief. For example, at 100 °C $Ga(HPO_4)_2F{\cdot}(NH_3(CH_2)_3NH_3){\cdot}2H_2O$ begins to disappear after 40 min of heating, and after only 5 min pure ULM-3 is observed.

Discussion and Conclusions

It is apparent from our work and an inspection of the literature that the tancoite chain, denoted $[M(T\Phi_4)_2\Phi]_n$ (M = octahedral metal center, and Φ = O, OH, or F) in Hawthorne's classification[36] is a common motif in phosphate chemistry and may be formed over a range of reaction conditions for a number of metals with oxidation state +3 (Al, Ga, Fe, V). We have produced two new compounds containing the same $Ga(HPO_4)_2F^{2-}$ chain, and both were prepared using milder conditions than typically used in the preparation of phosphates. The tancoite chains only contain 6-coordinate gallium, whereas it is well-known that in gallium phosphates prepared using hydrothermal methods gallium can be found in 4-, 5-, and 6-coordinate sites (or mixtures).[4] Leech et al. have recently studied the crystal growth at room temperature of aluminum and gallium phosphates using an organic template in silica gel.[37] The resulting structures also exhibit a metal:phosphorus ratio of 1:2, and the metal atom is also exclusively octahedrally coordinated. In these compounds the $[MO_6]$ octahedra are linked to four phosphate groups, and each octahedral metal is isolated from the others by the bridging phosphates. This connectivity results in layered structures of composition $[M(HPO_4)_2(H_2O)_2]$. The formation of compounds with low-dimensional structures and MP_2 stoichiometry appears to be favored for the gallium (or aluminum)−phosphate−amine system at ambient temperature. Further examples must be synthesized and characterized to confirm this suggestion.

The transformation of the fibrous $Ga(HPO_4)_2F{\cdot}(NH_3(CH_2)_3NH_3){\cdot}2H_2O$ to the three-dimensional framework ULM-3 is not direct and requires bond breaking and then reconstruction processes. The GaP_2 compound consists of infinite octahedral gallium chains, whereas the ULM-3 is composed of 5- and 6-fold coordinated gallium trimers isolated by phosphate groups. Furthermore, the different Ga:P, Ga:F, and Ga:amine stoichiometries for the starting gallium phosphate (Ga:P = 1:2; Ga:F = 1:1; Ga:amine = 1:1) and the final one (Ga:P = 1:1; Ga:F = 3:2; Ga:amine = 3:1) imply that the formation of the ULM-3 therefore involves a total structural reorganization. In situ EDXRD shows the dissolution of the chain phase, and this is almost complete before ULM-3 appears, consistent with a solution construction of ULM-3. The precursor $Ga(HPO_4)_2F{\cdot}(NH_3(CH_2)_3NH_3){\cdot}2H_2O$ thus plays the role of sole source of reactants, but not all species produced on dissolution are necessary for the formation of ULM-3, and this is consistent with the low pH of the supernatant liquid after reaction. Previous in situ NMR experiments performed on the AlPO system showed that the coordination of aluminum which is 6 at room temperature decreases to 5 in hydrothermal conditions and the pH also changes from acidic to neutral.[8] The metal coordination modification seen in the hydrothermal transformation of **1** into ULM-3, where we observe the formation of a compound containing both 5- and 6-coordinate Ga from one containing only 6-coordinate Ga, agrees with the NMR results.

This mechanistic scheme is quite different from that proposed by Ozin and co-workers for the formation of AlPO's.[5] They envisage that a linear chain is the basic building unit which undergoes successive arrangements (under hydrothermal conditions) to form a layered structure and finally a 3D network. In their hypothesis, each step requires only the breaking and creation of a few bonds, and chain-to-chain transformations are possible. The coordination state of aluminum remains tetrahedral for all the isolated products, and structural relationships with the parent chain are easily deduced from the observations of the AlP_2 linear chain within the topology of the final structures. In our system, the

(36) Hawthorne, F. C. *Am. Mineral.* **1985**, *70*, 455.

(37) Leech, A. M.; Cowley, A. R.; Prout, K.; Chippindale, A. M. *Chem. Mater.* **1998**, *10*, 451.

transformation of the chain to the 3D phase would not perhaps be predicted and is not obvious by considering the structures of the materials. The role of the hydrothermal treatment is critical and illustrates the complexities of the processes occurring in solution during a hydrothermal crystallization.

The transformation of open-framework structures into new phases is well-known in aluminosilicate zeolite chemistry. For example, zeolite Y (faujasite) will transform into zeolite P (gismondine) or ZSM-4 (mazzite), on extended periods of heating in solution,[38] and zeolite A will transform into zeolite P[39] or sodalite[40] on hydrothermal treatment with sodium hydroxide solution. As with the tranformations we report in this paper, the nature of the solution and the precise reaction conditions used to affect the transformation are of the utmost importance in the course of reaction achieved. Recently Tuel studied layered aluminosilicates observed in the synthesis of ZSM-48 and zeolite β, and concluded that these low-dimensional materials dissolve in the reaction conditions to provide aqueous species for zeolite crystallization.[41] This is analogous to the process we have described in this paper. The study of these hydrothermal transfomations clearly has a role to play in a better understanding of the crystallization mechanism of microporous materials.

Acknowledgment. We thank the Novartis Trust Fund for financial support and the EPSRC for provision of beam time at Daresbury.

CM000195+

(38) Barrer, R. M. *Hydrothermal Chemistry of Zeolites*; Academic Press: London, 1982.
(39) Subotic, B.; Smit, I.; Madzija, O.; Sekovanic, L. *Zeolites* **1982**, *2* 135.
(40) Subotic, B.; Skrtic, D.; Smit, I.; Sekovanic, L. *J. Cryst. Growth* **1980**, *50*, 498.
(41) Tuel A. *Chem. Mater.* **1999**, *11*, 1865.